



OPEN

Sauropodomorph evolution across the Triassic–Jurassic boundary: body size, locomotion, and their influence on morphological disparity

Cecilia Apaldetti^{1✉}, Diego Pol², Martín D. Ezcurra³ & Ricardo N. Martínez⁴

Sauropodomorph dinosaurs were the dominant medium to large-sized herbivores of most Mesozoic continental ecosystems, being characterized by their long necks and reaching a size unparalleled by other terrestrial animals (> 60 tonnes). Our study of morphological disparity across the entire skeleton shows that during the Late Triassic the oldest known sauropodomorphs occupied a small region of morphospace, subsequently diversifying both taxonomically and ecologically, and shifting to a different and broader region of the morphospace. After the Triassic–Jurassic boundary event, there are no substantial changes in sauropodomorph morphospace occupation. Almost all Jurassic sauropodomorph clades stem from ghost lineages that cross the Triassic–Jurassic boundary, indicating that variations after the extinction were more related to changes of pre-existing lineages (massospondylids, non-gravisaurian sauropodiforms) rather than the emergence of distinct clades or body plans. Modifications in the locomotion (bipedal to quadrupedal) and the successive increase in body mass seem to be the main attributes driving sauropodomorph morphospace distribution during the Late Triassic and earliest Jurassic. The extinction of all non-sauropod sauropodomorphs by the Toarcian and the subsequent diversification of gravisaurian sauropods represent a second expansion of the sauropodomorph morphospace, representing the onset of the flourishing of these megaherbivores that subsequently dominated in Middle and Late Jurassic terrestrial assemblages.

The diversification and radiation of dinosaurs in the early Mesozoic (Late Triassic–Early Jurassic, ~233–174 million years ago [Ma]) was one of the major biological events in the evolution of terrestrial vertebrates^{1–4}. During the Late Triassic, dinosaurs and pseudosuchians exploited similar resources and shared ecological roles in continental ecosystems^{5–7}. However, at the end-Triassic occurred a catastrophic event recognized as one of the ‘big five’ Phanerozoic mass extinctions^{8,9}, known as the end-Triassic extinction event (ETE). Causal hypotheses of this event range from gradualistic (sea-level fluctuations, widespread aridification) to catastrophic processes (e.g., bolid impact, volcanism)^{9–13}. After the Triassic–Jurassic boundary (TJB) all non-crocodylomorph pseudosuchians and non-dinosaurian dinosauromorphs went extinct, whereas most pre-existing dinosaur lineages survived, rapidly diversified, and prevailed during the subsequent 135 Myr of the Mesozoic Era^{1,2,4,7,8,14}. The precise pattern of change in terrestrial ecosystems across this boundary is still poorly understood, and current data suggests it was a result of a complex combination of events at different geographical scales, rather than a single mass extinction event^{3,15,16}.

Sauropodomorpha was the most diverse and abundant dinosaur clade at the time of the TJB, as this clade was the first dinosaur group that radiated and became both broadly distributed worldwide and dominant in Late Triassic continental ecosystems^{17,18}. Early sauropodomorphs first appeared during the Carnian (~233–231 Ma)

¹CONICET-IMCN, Instituto Y Museo de Ciencias Naturales-CIGEOBIO, Universidad Nacional de San Juan, Av. España 400 Norte, 5400 San Juan, Argentina. ²CONICET-MEF, Museo Paleontológico Egidio Feruglio, Av. Fontana 140, Trelew, Chubut, Argentina. ³CONICET-MACN, Sección Paleontología de Vertebrados, CONICET-Museo Argentino de Ciencias Naturales “Bernardino Rivadavia”, Av. Ángel Gallardo 470, C1405DJR Ciudad Autónoma de Buenos Aires, Argentina. ⁴Instituto Y Museo de Ciencias Naturales (IMCN)-CIGEOBIO, Universidad Nacional de San Juan, Av. España 400 Norte, 5400 San Juan, Argentina. ✉email: capaldetti@unsj.edu.ar

and later diversified to become the most abundant component of dinosaur faunas during approximately 30 million years (Myr) (Norian–Pliensbachian; ca. 220–190 Myr^{17,19}). These diverse early sauropodomorph lineages were replaced at the end of the Early Jurassic (Toarcian, ~180 Ma) by Gravisauria²⁰, a clade that includes giant quadrupedal sauropods that were the largest land vertebrates to inhabit the Earth^{18,21–26}. The known taxonomic and morphological diversity of early sauropodomorphs has dramatically increased in recent years^{27–33}, providing critical new information on their evolution during a long period of ecological dominance (Norian–Pliensbachian). Research efforts during the last decade yielded certain consensus on the phylogenetic hypotheses of this group^{27–37}, but global ecomorphological aspects have been explored only recently^{38–40}. Here, we evaluate quantitatively the evolutionary history of Sauropodomorpha through a comprehensive morphological disparity analysis and regression-based phylogenetic comparative methods of the entire skeleton that allows us characterizing certain aspects of the macroevolution of the group during the Late Triassic and Early Jurassic.

Results

Carnian sauropodomorphs had an initial diversification restricted to a limited and well-differentiated region of the morphospace, representing the small, bipedal and highly plesiomorphic sauropodomorph body plan (Fig. 1a,b). Our results (significant differences between disparity metrics were calculated after determining the non-overlapping of 95% confidence intervals generated from 9,999 bootstrap replicates; see “Methods”) show an increase in morphospace size and density from the origin of the group (Carnian) towards the Jurassic (Figs. 1, 2). This is shown by the increase in weighted mean pairwise dissimilarity (WMPD, a pre-ordination metric that captures mainly morphospace density) as well as in the Sum of Ranges (SoR) and Sum of Variances (SoV) (post-ordination metrics that captures morphospace size and density, Table 1; see “Methods”).

The morphological disparity (WMPD) and the amount of morphospace occupied (SoR) significantly increase by the Norian–Rhaetian (Figs. 1a,c, 2a,b; Table 1), documenting the main diversification of early sauropodomorphs. Most early sauropodomorph lineages (plateosaurids, riojasaurids, massospondylids, sauropodiforms) appeared between the mid-Norian (~215 Ma) and the end-Triassic (~201 Ma)^{33,34,38,41}. This large diversification of sauropodomorphs and the associated anatomical novelties position these forms in a previously unexplored region of the morphospace. This position shift is documented by significant results in the displacements from the centroid, which is a post-ordination metric that captures differences in morphospace position (Fig. 2c; Table 1), and a permutational multivariate analysis of variance ($p < 0.01$ in a PERMANOVA) between the first two analysed time bins. Extremes of the different body shapes and sizes recorded during the Norian–Rhaetian include the facultatively bipedal early plateosaurians (i.e., *Plateosaurus*, *Unaysaurus*)⁴², and the larger, robust, and quadrupedal sauropodiforms (e.g., lessemsaurids)^{28,29,37,43,44}. The gracile *Nambalia* and *Jaklapalisaurus* enlarge the region of the morphospace overlapping with some Carnian forms in the first two principal coordinates (i.e., *Eoraptor*, *Saturnalia*), whereas some Rhaetian forms (*Thecodontosaurus*, *Pantydraco*) are closely positioned to *Panphagia* in these same coordinates (Fig. 2b).

Immediately after the TJB the morphological disparity (WMPD) of Sauropodomorpha has a minor increase (which is only marginally significant after the exclusion of taxa that had to be trimmed for the ordination of the dataset; see Methods), coupled with a slight increase of the amount of morphospace occupied (SoR) (Figs. 1a,d, 2a; Table 1). The diversity of the earliest Jurassic sauropodomorphs includes members of most early massopodan clades and a large number of ghost lineages subtending Early Jurassic taxa^{28,29,33,38}, which indicates that no major clades originated at this time (Fig. 1). In agreement, the morphospace occupied by Early Jurassic sauropodomorphs largely overlaps that of the latest Triassic forms and there is a minor, marginally significant occupation of new areas of the morphospace during this period (displacements from centroid and $p = 0.0117$ in a PERMANOVA; Fig. 2c; Table 1). This result is in accordance with previous results based on a subset of the taxa analysed here³⁸ and two-dimensional geometric morphometrics of the cranium and pelvic girdle⁴⁵.

Post-Toarcian sauropodomorphs occupy a significantly different area of the morphospace with respect to that of previous time bins (as reflected in the displacements from centroid and $p < 0.001$ in PERMANOVAs; Table 1). There is also a slight decrease in the morphospace size and density (SoR and SoV) (Figs. 1a,e, 2b,c; Table 1). The new region of the morphospace occupied during the Toarcian–Middle Jurassic (Fig. 2c) represents the emergence of new lineages distinguished by a unique body plan (e.g., Vulcanodontidae, Gravisauria, Eusauropoda) of obligatory quadrupedal stance, elongated forelimbs, and columnar limbs, all features interpreted as related to their large body mass^{20,22,38} (Figs. 1a,e, 2d).

Procrustes-distance-based phylogenetic regressions indicate that these early evolutionary patterns of Sauropodomorpha are strongly influenced by the evolution of body mass ($R^2 = 0.4670$ and $p < 0.05$ in all the regressions of the first three PCos versus log(body mass); see Supplementary Information). A wide range of body shapes and sizes are recorded in Sauropodomorpha between the Carnian and the Middle Jurassic, including the gracile and bipedal early forms (*Saturnalia*, *Eoraptor*, < 50 kg), the facultatively bipedal early plateosaurians (e.g., *Efraasia*, *Unaysaurus*; ~100–1000 kg), the large and robust quadrupedal sauropodiforms (e.g., *Antetonitrus*, *Lessemsaurus*, *Ledumahadi*; > 5 tn), and the giant gravisaurian sauropods (e.g., *Vulcanodon*, *Bagualia*, *Patagosaurus*; > 10 tn) (Fig. 2d; Supplementary Information). A second variable that also explains a lower, but nonetheless considerable, amount of variance is the present-day continent occurrence of taxa ($R^2 = 0.3746$ and $p < 0.05$ in all the regressions of the first three PCos versus biogeography; see Supplementary Information). However, the interaction model between body mass and biogeography performed considerably worse than each variable independently ($R^2 = 0.2103$ and $p < 0.05$ for log(body size) and $R^2 = 0.1243$ and $p > 0.05$ for biogeography in all the regressions of the first three PCos versus log(body size) + biogeography; see Supplementary Information).

When the dataset was divided into four anatomical partitions (skull + dentition, vertebrae, pectoral girdle + forelimb, and pelvic girdle + hindlimb), a pattern of disparity increase through time (as captured by WMPD) is also recovered for skull + dentition and vertebrae, but the Toarcian–Middle Jurassic time bin was not

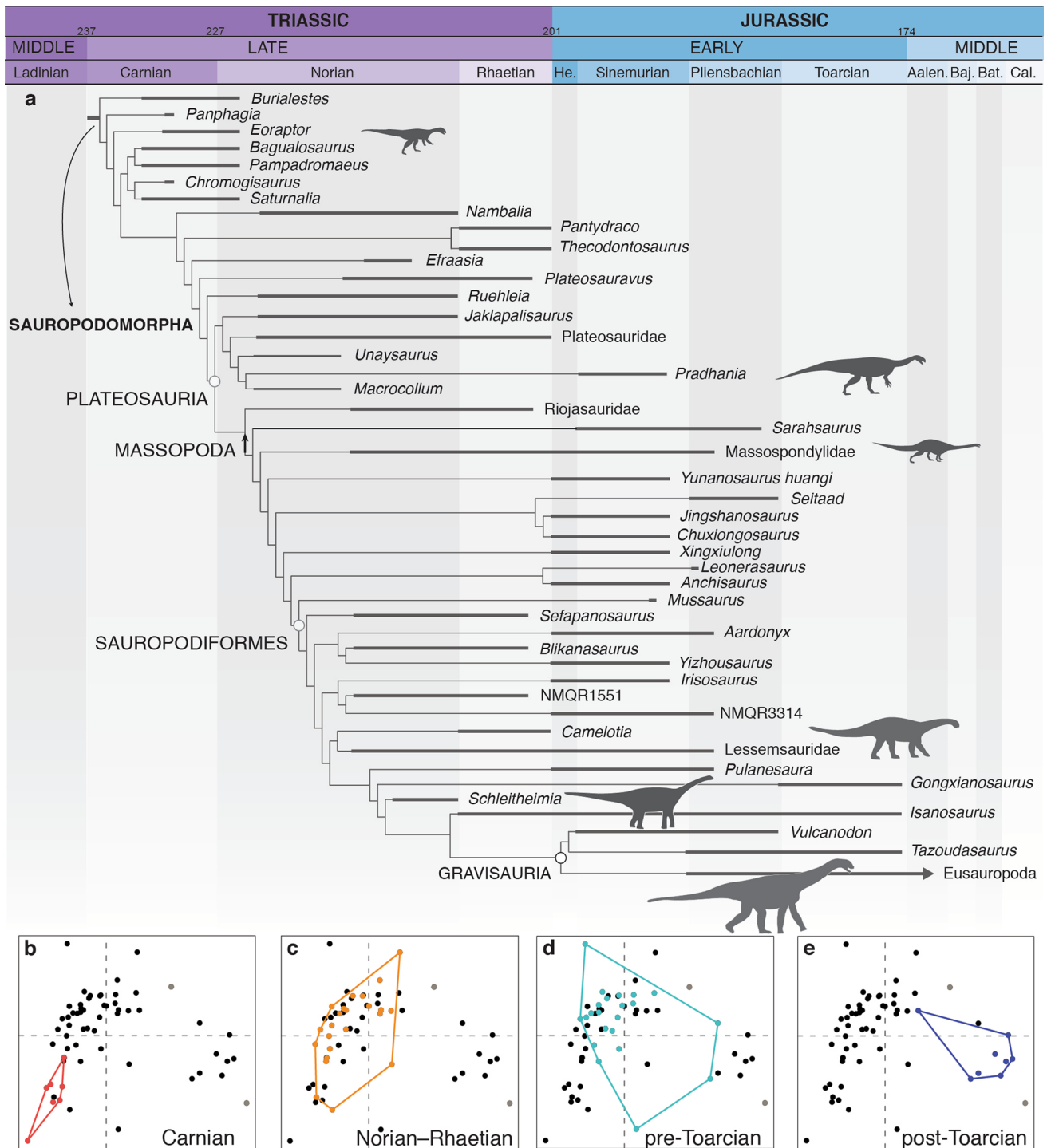


Figure 1. Morphospaces and diversity of Sauropodomorpha during the Triassic–Early Jurassic. **(a)** Randomly selected, time calibrated MPT and morphospace occupation of Sauropodomorpha during **(b)** Carnian, **(c)** Norian–Rhaetian, **(d)** pre-Toarcian, and **(e)** post-Toarcian periods. Each plot shows the first two principal coordinate axes, with a variance of 9.82% (PCo 1, x axis) and 3.90% (PCo 2, y axis) (see Fig. 2b for more details about morphospace plots).

significantly different from the pre-Toarcian bin (Supplementary Information). Interestingly, these two anatomical partitions have Jurassic WMPD values significantly higher than those of the Triassic, contrasting with the analyses for the whole skeleton that found non-significant changes across the TJB. The pectoral girdle + forelimb dataset has a relatively constant, non-significantly different, disparity (WMPD) from the Carnian to the Pliensbachian, but it drops significantly during the Toarcian–Middle Jurassic (Supplementary Information). A similar pattern is recovered for the pelvic girdle + hindlimb, in which the Toarcian–Middle Jurassic disparity (WMPD)

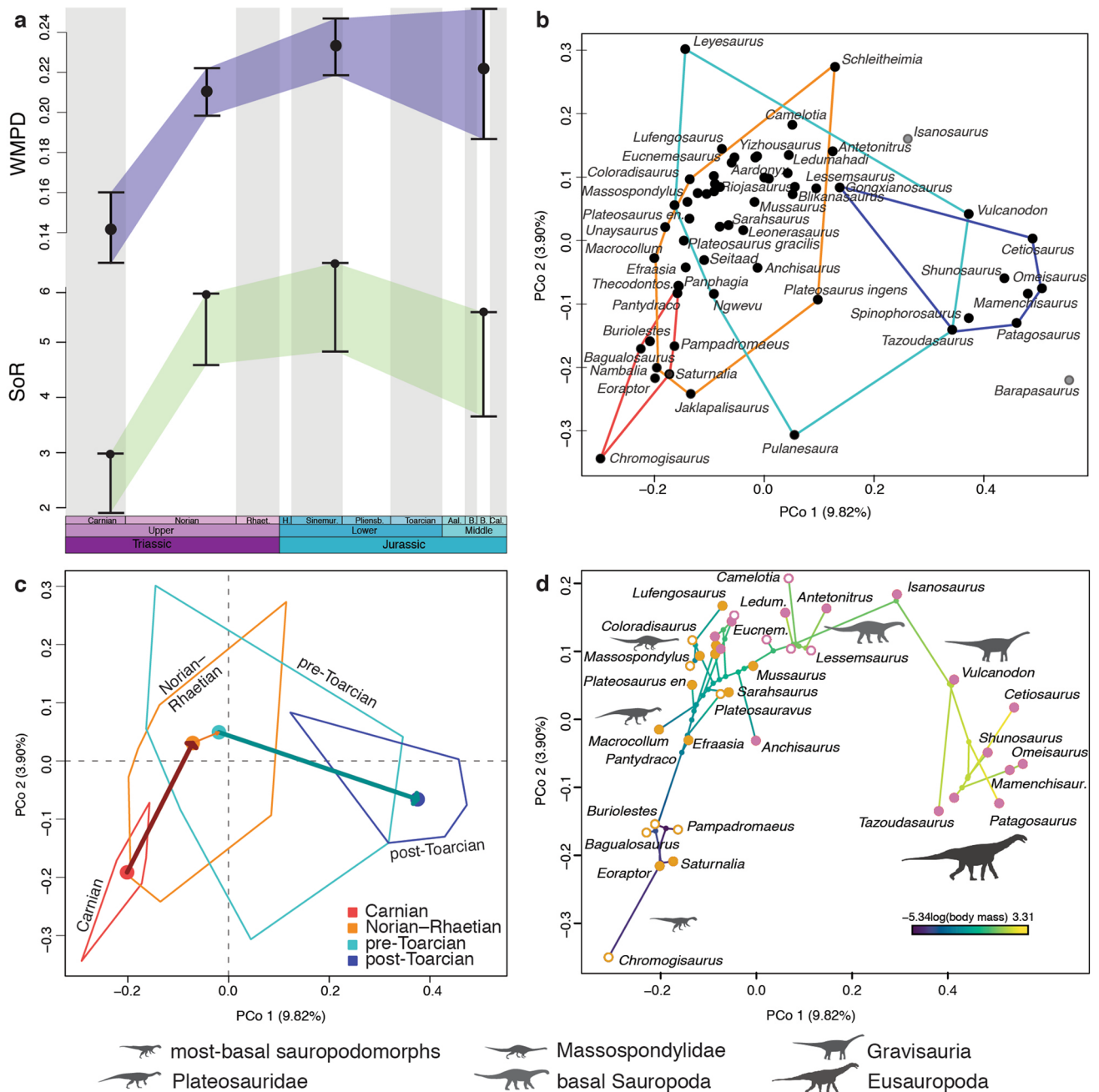


Figure 2. Morphological disparity of Sauropodomorpha during the Triassic–Early Jurassic. **(a)** Weighted mean pairwise dissimilarity (WMPD) and Sum of Ranges (SoR) with their respective 95% confidence intervals. **(b)** Morphospace distribution in the first two PCOs. *Barapasaurus* and *Isanosaurus* (greys circles) were excluded from time bin groups because their temporal uncertainty. **(c)** Displacement from the centroid of the previous time bin, in which the thickness of the arrows is proportional to the multidimensional distance of the displacement. **(d)** Phylomorphospace showing locomotion style (mapped in orange circles for bipedal and pink circles for quadrupedal) and body mass optimized through time (colours of branches). Empty circles represent assumed locomotion style based on Fitch optimization in the phylogenetic trees.

is significantly lower and marginally lower than the pre-Toarcian and Norian–Rhaetian time bins, respectively. The Carnian WMPD value of the pelvic girdle + hindlimb region is significantly lower than that around the TJB, but non-significantly lower than during the Toarcian–Middle Jurassic.

Discussion and conclusion

At the time of its first appearance in the fossil record (middle–late Carnian), sauropodomorphs were first restricted to a few small species (so far exclusively found in South America and preliminary reported in Africa^{33,46}). This early stage in sauropodomorph evolution is characterized by low morphological disparity

Bin	WMPD	Lower limit	Upper limit
WMPD all taxa			
Carnian	0.1419317	0.1246697	0.1591733
Norian–Rhaetian	0.2143386	0.2021589	0.2257176
Pre-Toarcian	0.2494814	0.2339706	0.2639456
Toarcian–MJ	0.2188413	0.1898161	0.2449658
WMPD locomotion			
Bipeds	0.2231127	0.2143411	0.2320984
Quadrupeds	0.3280687	0.3117793	0.3442396
Bin	SoV	Lower limit	Upper limit
SoV all taxa			
Carnian	0.1057576	0.09002641	0.1590102
Norian–Rhaetian	0.1580963	0.12401888	0.2046489
Pre-Toarcian	0.1831581	0.14149178	0.2421437
Toarcian–MJ	0.2246976	0.21185220	0.2951077
SoV locomotion			
Bipeds	0.1356129	0.1088801	0.1708456
Quadrupeds	0.2089300	0.1845635	0.2493610
Bin	SoR	Lower limit	Upper limit
SoR all taxa			
Carnian	3.658997	2.220012	3.658997
Norian–Rhaetian	6.750165	5.186897	6.750165
Pre-Toarcian	7.360617	5.563492	7.360617
Toarcian–MJ	6.327877	4.421535	6.327877
SoR locomotion			
Bipeds	6.760765	4.988128	6.760765
Quadrupeds	7.959643	6.582425	7.959643
Bin	Displacement	Lower limit	Upper limit
Displacement from centroid all taxa			
Carnian	1.518088	1.452325	2.312874
Norian–Rhaetian	1.063757	1.035988	1.162953
Pre-Toarcian	1.045143	1.016389	1.130591
Toarcian–MJ	1.364435	1.279873	1.751107
Displacement from previous time bin			
Carnian	1.000000	1.000000	1.000000
Norian–Rhaetian	1.425361	1.337646	1.581720
Pre-Toarcian	1.092128	1.058417	1.189740
Toarcian–MJ	1.376450	1.292433	1.774152
Displacement from centroid of locomotion styles			
Bipeds	1.115236	1.082434	1.206832
Quadrupeds	1.018242	1.010159	1.074852

Table 1. Selected results of the morphological disparity analyses (all other results are reported in the supplementary information). The upper and lower limits were calculated after building 95% confidence intervals calculated from 9999 bootstrap replicates of the distance (WMPD) and ordinated matrices (other measures). Abbreviations: MJ, Middle Jurassic.

(Figs. 1, 2a; Table 1). However, small and bipedal taxa with a plesiomorphic body plan were not restricted to the Carnian, as the Norian *Nambalia*⁴⁷ and the Rhaetian *Thecodontosaurus* and *Pantyraco*⁴⁸ share many features and occupy a similar region of the morphospace (Figs. 1, 2b). These Rhaetian taxa are also positioned in a similar region of the morphospace even when only feeding-related features of the jaw apparatus are assessed⁴⁰.

Body size explains approximately half of the variance in our analysis (first three PCos) and, in congruence, the Carnian–Norian shift detected in the morphospace of Sauropodomorpha (Figs. 1a–c, 2c) is consistent with the Norian rapid initial diversification^{3,33,38,49} or early burst pattern inferred in studies of dinosaurian body size evolution^{25,50}; sauropodomorph body mass increase from around < 50 kg in Carnian forms to > 5 tonnes in some Norian sauropodiforms²⁸. This early shift likely involved an increase in morphological evolutionary rates that allowed the group to diversify, developing different body plans and occupying disparate ecological niches^{38,39,50}, after the Carnian–Norian boundary. A significant shift in morphospace between the Carnian and Norian is also congruent with changes in feeding behaviour inferred between the Carnian taxa (e.g., possible faunivorous taxa

as *Saturnalia* or *Buriolestes*) and the omnivorous to herbivorous lifestyle adaptations present in later Triassic taxa (e.g., plateosaurians)^{38–41,51}. The wide expansion of the Norian morphospace highlights the main diversification of early sauropodomorphs during mid-Norian and the end-Triassic, when most early lineages appeared (plateosaurids, riojasaurids, massospondylids, sauropodiforms)^{33,34,38,41}. This great expansion of morphospace of Sauropodomorpha during the Norian probably evidence the occupation of new niches that were exploited by other herbivorous groups previous to the TJB (such as rhynchosaurs, large traversodontid cynodonts, and dicynodonts)^{1,7,14,38,52,53}.

The major radiation of Sauropodomorpha in the Norian^{3,50,54} is evidenced not only in the increase in their taxonomic diversity and geographic distribution, but also in adaptive changes that goes beyond dietary habits. A marked increase in body size occurs during this stage, coupled with the acquisition of the early sauropodomorph body plan, characterized by small head, elongated neck, three sacral vertebrae, and a modified first manual digit^{17,24,33,38,39,55}. All these changes explain the shift and dramatic expansion of their morphological disparity during Norian times (Figs. 1, 2a–c). In parallel to these changes, sauropodomorphs became numerically dominant in terrestrial ecosystems^{1,3,19,38,54} and were not restricted mostly to South America anymore, occurring with several species in Europe, India and Africa^{2–4,19,38,47,56}. As a result of this and the subsequent appearance of sauropodomorphs in North America and Asia only after the TJB, our regression analyses find that the biogeographic distribution of species partially matches the morphospace pattern. The anatomical changes that underlie the major disparity excursions of sauropodomorphs in this transition seem to have also strongly influenced disparity changes detected in Dinosauria as a whole^{7,14}.

Sauropodomorpha was the most diverse group of terrestrial herbivores across the TJB and our analyses show there were no major changes in their ecomorphology throughout that time (Figs. 1 and 2a). A similar result was also obtained in analyses of morphological disparity and biomechanical properties of sauropodomorph jaws^{39,45}. Other analyses, based on a subset of the taxa analysed here, recovered only a slight increase or a shift in the morphospace occupation of Sauropodomorpha across the TJB^{38,40}. Sauropodomorph diversity has been regarded as decreasing worldwide after the TJB^{14,57–60}, but recent discoveries in the Early Jurassic^{27,29,31,32} indicate a higher diversity to levels similar to those of the Late Triassic. Moreover, the greater diversity of sauropodomorphs now known for the upper Elliot Formation of South Africa reflect their abundance and increase in morphological disparity after the TJB^{19,38}, suggesting that the mass extinction did not negatively affect Sauropodomorpha^{29,37,61}. Indeed, the increase in skull and vertebral disparity from the Late Triassic to the earliest Jurassic in our results indicates there were changes probably related more diverse trophic habits and an increase in the complexity of vertebral lamination and pneumaticity, which are anatomical regions that were already subject to numerous evolutionary changes during the Triassic in sauropodomorphs^{28,41,62,63}. Thus, the events across the TJB in sauropodomorph evolution likely were a continuity of evolutionary trends in pre-existing lineages (massospondylids, non-gravisaurian sauropodiforms) rather than representing the emergence of key evolutionary novelties or new, considerably different, body plans. A noteworthy difference across the boundary is the disappearance of small-bodied sauropodomorphs (extended from the earliest sauropodomorphs as *Panphagia* to the latest Triassic forms as *Thecodontosaurus* or *Pantyraco*)⁶¹.

Finally, a major event in sauropodomorph evolution is the diversification of gravisaurian sauropods, implying numerous changes in their body plan, locomotion, feeding behaviour, and extremely large body size^{20,22–24,39,40,55}. This event represents a second expansion of morphospace towards previously unexplored regions (Figs. 1, 2c), and reflects the significant body plan changes of Sauropodomorpha at this time. At the same time, the significantly lower Toarcian–Middle Jurassic disparity values of the pelvic girdle and hindlimb is probably related to the extinction of non-sauropodan sauropodomorphs by the late Pliensbachian^{20,38} that left gravisaurian sauropods as the only surviving sauropodomorphs. This same pattern has been recovered for the pelvic girdle using geometric morphometrics, but not for the cranium⁴⁵. The large size, obligatory quadrupedality and graviportality of sauropods likely imposed morphofunctional constraints that restricted the morphospace occupation in this anatomical region. From an ecological point of view, it has been noted that the diversification of “broad-crowned” early sauropods implied a functional shift of the feeding apparatus toward greater cranial robustness and bite force^{20,39,41}. This is consistent with the significantly higher skull disparity values after the TJB and the adoption of obligate high-fiber herbivory³⁹, in comparison to the condition present in earlier Sauropodiformes.

The change in locomotion style (bipedal to quadrupedal) and the successive increase in body mass that characterizes Sauropodomorpha over time (Fig. 2d), associated with the acquisition of a fully herbivorous diet (with increased bite force and cranial robustness)^{39,40,51,64}, have been found here to be the main attributes responsible for the distribution of Triassic to Middle Jurassic species in the morphospace. A clear pattern is that the disparity of sauropodomorphs radically shifted twice: first after the Carnian/Norian boundary, when plateosaurians radiated^{33,38}, and later by the end of the Early Jurassic^{22,40,65}, when all non-sauropod sauropodomorphs went extinct and gravisaurians became the predominant megaherbivores during the rest of the Mesozoic Era²⁰.

Methods

Data matrix and phylogenetic analysis. Our analyses are based on a comprehensive phylogenetic dataset available for Late Triassic–Early Jurassic Sauropodomorpha³³, composed of 79 taxa and 419 characters. An equally weighted parsimony analysis in TNT 1.5⁶⁶ resulted in 820 most parsimonious trees (MPTs) of 1693 steps (see electronic supplementary material).

Time bins and calibrated phylogenies. In order to analyse evolutionary patterns of Sauropodomorpha across the TJB we used four time bins: Carnian (233.2–225.7 Ma), Norian–Rhaetian (225.7–201.3 Ma), pre-Toarcian Jurassic (201.3–182.7 Ma), and Toarcian–Middle Jurassic (182.7–163.5 Ma). All the 820 MPTs were time-calibrated with the timePaleoPhy() function of the R package paleotree⁶⁷, using the ‘mbf’ method⁶⁸ with a

minimum branch length of 0.1 (Supplementary Data File). These time-calibrated trees were used for the regression analyses and the phylomorphospace plots (see below). We have not used other alternative minimum branch lengths or stochastic calibration methods (e.g., 'cal3') because of computational time limitations; 31 regressions, each with 999 iterations, were conducted for each of the 820 trees, resulting in a total of > 25,000,000 runs.

Morphological disparity analyses. Morphological diversity (disparity) was quantified using the R package Claddis v0.6.3⁶⁹. All non-sauropodomorph terminals and the suprageneric Neosauropoda were excluded before the analyses, resulting in a final dataset of 67 species-level terminals. Morphological disparity was compared between time bins, biped/quadruped locomotion categories (first, using a reduced sample of taxa with locomotion style inferred only from humerus-femur circumference ratio²⁹, and second, a broader sample including the latter plus other taxa whose locomotion style was estimated here from a Fitch optimization in the most parsimonious trees), and skull + dentition/vertebrae/pectoral girdle + forelimb/pelvic girdle + hindlimb categories. Three terminals occur across two or three of our a priori selected time bins because of chronostratigraphic uncertainty of the rocks units where they were found (*Isanosaurus*, *Barapasaurus* and *Tazoudasaurus*). These taxa were considered in all possible time bins in the disparity analyses, but sensitivity analyses pruning *Isanosaurus* and *Barapasaurus* were conducted because of their more distant position to where most species occur in the first three axes of the ordinated morphospace. The distance matrix was generated from the taxon-character data matrix using the Maximum Observable Rescaled Distance (MORD⁶⁹) because the commonly used Generalized Euclidean Distance (GED) may produce a strong methodological bias in matrices with a moderate to high amount of missing data^{70–72}. Indeed, this is the case in our dataset, in which there is a significant correlation ($p < 0.001$; Pearson's product-moment correlation) between the distance from the centroid and the amount of missing data of each taxon. The distance matrix was used to calculate the pre-ordination metric weighted mean pairwise dissimilarity (WMPD) for all temporal, locomotion, and skeletal groups in order to capture density of each analysed group⁷³. We used WMPD because it allows analysing the dataset with all taxa regardless of trimmings necessary for the ordination of the distance matrix.

An ordination of the distance matrix was performed using a Principal Coordinates Analysis (PCoA) with Lingoes correction because of the presence of negative eigenvalues. Six species (*Xixipiosaurus suni*: 84.2% missing data; *Chuxiongosaurus lufengensis*: 84.7%; *Pradhania gracilis*: 94.5%; *Ingentia prima*: 90.4%; *Meroktenos thabanensis*: 90.2%; *Glacialisaurus hammeri*: 92.8%) had to be trimmed to conduct the ordination because of the absence of overlapping scored characters between pairs of taxa. MORD may generate a methodological artefact of repulsion from the centroid of terminals with high amount of missing data^{72,74}. We visually identified four of these 'outliers' in the first four coordinates (*Chromogisaurus*: 86.16% missing data; *Jaklapallisaurus*: 91.65%; *Plateosaurus ingens*: 94.75%; *Pulanesaura*: 83.53%). We calculated four post-ordination disparity measures with the intention to comprehensively describe the multidimensional morphospace: Sum of Variances (SoV), Sum of Ranges (SoR), and mean displacements from the centroid either with respect to the centroid of the complete dataset or with respect to the previous time bin. We tested how each of these measures captures three different aspects of the morphospace (size, density and position) using the test.metric function of the dispRity package^{73,75}, following the simulations of Guillerme et al.⁷³. Sum of Variance successfully captured both size (inner size slope = 1.590743e-03 and outer size slope = -1.499010e-03) and density (higher density slope = 1.501165e-03 and lower density slope = -1.888993e-03), but not position (top position slope = -7.066390e-04 and bottom position slope = -1.137366e-04). Sum of Ranges also successfully captured size (inner size slope = 0.07676521 and outer size slope = 0.02702388) and density (higher density slope = 0.07122427 and lower density slope = 0.01671752), but not position (top position slope = 0.03571710 and bottom position slope = 0.03657908). In particular, the proportionally higher inner size slope of Sum of Ranges indicates that this metric was more sensitive to size contraction than Sum of Variances. Finally, the mean displacements from the centroid of all the dataset did not show a good performance for any particular morphospace trait, but it detected position differences when 30% or more of the original data was considered. As a result, in order to complement this metric, the presence of different morphospace positions was tested with PERMANOVA tests among the different temporal categories (with 9,999 permutations, using the 'euclidean' method, and excluding *Barapasaurus* and *Isanosaurus*). All the post-ordination measures were calculated with functions of the dispRity package^{73,75} and the PERMANOVA was conducted with the adonis function of the vegan package⁷⁶. All these calculations and tests were conducted using the first 17 coordinates (45.91% of accumulated variance) that were chosen by graphically exploring the scree plot of percentages of explained variance for each coordinate and detecting the last major change of slope in the curve. All the post-ordination metrics were calculated for the complete ordinated data set, and the ordinated data set without 'outliers' and without 'outliers' and *Barapasaurus* and *Isanosaurus*. In order to compare the pre-ordination and post-ordination results, we calculated the WMPD also for the dataset without the six species that were necessary to trim to conduct the ordination and without *Barapasaurus* and *Isanosaurus*.

Statistical significance between groups was assessed through the non-overlap of 95% confidence intervals calculated from 9999 bootstrap replicates (boot.matrix() function of dispRity) of the dissimilarity matrix for WMPD and the ordinated matrix for the post-ordination disparity metrics, and the subsequent recalculation of the measures. We used an odd number of bootstrap replicates in order to have all values within the two population tails. The 95% confidence intervals were generated using the two tails (0.025%) of the population of values recovered from the resampled matrix. This procedure was followed by all the disparity metrics with the exception of Sum of Ranges, because in this one the resampled values cannot be higher than the original value of the non-resampled dataset. As a result, in the case of Sum of Ranges we used only one tail (0.05%) of the population of resampled values to build the 95% confidence intervals. In addition, we calculated the rarefied and non-rarefied (to seven elements, which is the minimum taxonomic sample among the time bins) confidence intervals for the three post-ordination disparity measures, when analysing the complete dataset, in order to explore how sensitive

our dataset is to differences in sample. We have not detected differences in the significance of the results between both methods. These resamples of the original dataset and the analyses including and excluding outlier taxa allow accounting for sample size differences among the different dataset partitions.

Morphospace and phylomorphospace bivariate plots (PCo1 versus PCo2) were generated based on the results of the PCoA (see electronic supplementary material). Phylomorphospaces were created using one, randomly selected time-calibrated tree and the continuous character log(body mass) was mapped, using a maximum likelihood optimization, in one of these phylomorphospaces using the `contMap()` and `phylomorphospace()` functions of the R package `phytools`⁷⁷.

Regression-based phylogenetic comparative analyses. The relationship between the first three coordinates of the morphospace and different explanatory variables, and several of their combinations (multi-model), were assessed using Procrustes-distance-based phylogenetic regressions⁷⁸ via the `procD.pgls` function (using type II sum of squares and 999 iterations) of the R package `geomorph`⁷⁹. We choose to use the first three PCos (16.87% of accumulated variance) because they are the only ones that explain more than 3% of the variance and the curve of the scree plot has its major inflexion point between the PCo3 and PCo4. This regression-based analyses are very sensitive to conflictive information that usually occur in larger PCos with a low amount of explained variance and as a result we decided to exclude them from these tests. These regressions were conducted for each of the 820 time-calibrated MPTs. These analyses included four numerical explanatory variables: (1) log(femoral length), (2) log(body mass), (3) log(humeral shaft circumference)/log(femoral shaft circumference), and (4) tree shape (calculated as the diagonal of the phylogenetic variance–covariance matrix of trees with all branch lengths equal to 1); and two categorical variables: (5) continent of occurrence and (6) locomotion style (biped | quadruped). Locomotion style and humeral–femoral circumferences ratio were used in a first (N = 24 and 15 different models) and a second (N = 36 and 16 different models) series of regressions, but not together, because the former variable has been used to infer the latter²⁹. Similarly, in the first series of regressions, log(femoral length) and log(body mass) were not considered together because both variables may covariate⁸⁰. In these regressions, we used the locomotion style of taxa inferred from the humeral–femoral circumference ratio²⁹, as well as those estimated here after a Fitch optimization. Regarding topological structure (or phylogenetic structure) as one of the explanatory variables, it is worth to explain that the diagonal of the phylogenetic variance–covariance matrix of a tree with all equal length branches produces a vector with the number of nodes between each terminal taxon and the root of the tree. As a result, this vector describes quantitatively the topology of the phylogenetic tree and it is not equivalent to the diagonal of the variance–covariance matrix generated from the time-calibrated tree that was used to describe the heteroscedasticity of the dataset. The output of the `procD.pgls` function does not allow to calculate the Akaike's information criterion; thus, the different models were compared between each other based on their R² and p values (see electronic supplementary material).

Data availability

Morphological disparity analyses, R scripts and data matrices are available in the Supplementary data files.

Received: 28 January 2021; Accepted: 21 October 2021

Published online: 18 November 2021

References

- Benton, M. J. Origin and relationships of Dinosauria. In *The Dinosauria* (eds Weishampel, D. B. *et al.*) 7–19 (University of California Press, California, 2004).
- Langer, M. C., Ezcurra, M. D., Bittencourt, J. S. & Novas, F. E. The origin and early evolution of dinosaurs. *Biol. Rev.* **85**, 55–110 (2010).
- Irmis, R. B. Evaluating hypotheses for the early diversification of dinosaurs. *Earth Environ. Sci. Trans. R. Soc. Edinb.* **101**, 397–426 (2011).
- Brusatte, S. L. *et al.* The origin and early radiation of dinosaurs. *Earth Sci. Rev.* **101**, 68–100 (2010).
- Benton, M. J. Dinosaur success in the Triassic: A noncompetitive ecological model. *Q. Rev. Biol.* **58**, 29–55 (1983).
- Charig, A. J. Competition between therapsids and archosaurs during the Triassic Period: A review and synthesis of current theories. *Symp. Zool. Soc. Lond.* **52**, 597–628 (1984).
- Brusatte, S. L., Benton, M. J., Ruta, M. & Lloyd, G. T. Superiority, competition and opportunism in the evolutionary radiation of dinosaurs. *Science* **321**, 1485–1488 (2008).
- Benton, M. J. Diversification and extinction in the history of life. *Science* **268**, 52–58 (1995).
- Olsen, P. E. *et al.* The continental Triassic–Jurassic boundary in central Pangea: Recent progress and preliminary report of an Ir anomaly. In *Catastrophic Events and Mass Extinctions: Impacts and Beyond* (eds Koerberl, C. & MacLeod, K. G.) 505–522 (Geological Society of America Special Papers, 2002).
- Olsen, P. E. *et al.* Ascent of dinosaurs linked to an iridium anomaly at the Triassic–Jurassic boundary. *Science* **296**, 1305–1307 (2002).
- Tanner, L. H., Lucas, S. G. & Chapman, M. G. Assessing the record and causes of Late Triassic extinctions. *Earth Sci. Rev.* **65**, 103–139 (2004).
- Whiteside, J. H., Olsen, P. E., Kent, D. V., Fowell, S. J. & Et-Touhami, M. Synchrony between the CAMP and the Triassic–Jurassic mass-extinction event?. *Palaeogeogr. Palaeoclimatol. Palaeoecol.* **244**, 345–367 (2007).
- Blackburn, T. J. *et al.* Zircon U–Pb geochronology links the end-Triassic extinction with the Central Atlantic Magmatic Province. *Science* **340**, 941–945 (2013).
- Brusatte, S. L., Benton, M. J., Ruta, M. & Lloyd, G. T. The first 50Myr of dinosaur evolution: Macroevolutionary pattern and morphological disparity. *Biol. Lett.* **4**, 733–736 (2008).
- Benton, M. J. What really happened in the Late Triassic?. *Hist. Biol.* **5**, 263–278 (1991).
- Du, Y. *et al.* The asynchronous disappearance of conodonts: New constraints from Triassic–Jurassic boundary sections in the Tethys and Panthalassa. *Earth Sci. Rev.* **203**, 103176. <https://doi.org/10.1016/j.earscirev.2020.103176> (2020).
- Galton, P. M. & Upchurch, P. Prosauropoda in *The Dinosauria* (eds Weishampel, D. B., Dodson, P. & Osmólska, H.) 232–258 (University of California Press, 2004).

18. Upchurch, P., Barrett, P. M. & Dodson, P. Sauropoda. In *The Dinosauria* (eds Weishampel, D. B., Dodson, P. & Osmólska, H.) 259–322 (University of California Press, 2004).
19. Bordy, E. M. *et al.* A chronostratigraphic framework for the upper Stormberg Group: Implications for the Triassic–Jurassic boundary in southern Africa. *Earth Sci. Rev.* **203**, 103120. <https://doi.org/10.1016/j.earscirev.2020.103120> (2020).
20. Pol, D. *et al.* Extinction of herbivorous dinosaurs linked to Early Jurassic global warming event. *Proc. R. Soc. B* **287**, 20202310. <https://doi.org/10.1098/rspb.2020.2310> (2020).
21. Barrett, P. M. & Upchurch, P. Sauropod diversity through time: Possible macroevolutionary and paleontological implications. In *The Sauropods: Evolution and paleobiology* (eds Curry-Rogers, K. A. & Wilson, J. A.) 125–156 (University of California Press, California, 2005).
22. Allain, R. & Aquesbi, N. Anatomy and phylogenetic relationships of *Tazoudasaurus naimi* (Dinosauria, Sauropoda) from the late Early Jurassic of Morocco. *Geodiversitas* **30**, 345–424 (2008).
23. Klein, N., Remes, K., Gee, C.T. & Sander, P. M. *Biology of the Sauropod Dinosaurs: Understanding the Life of Giants* (Indiana University Press, 2011).
24. Sander, P. M. (coord. author) Sauropod Gigantism: A Cross-Disciplinary Approach (PLoS ONE Collections, 2013).
25. Benson, R. B. J., Hunt, G., Carrano, M. T. & Campione, N. E. Cope's rule and the adaptive landscape of dinosaur body size evolution. *Palaeontology* **61**, 13–48 (2017).
26. Carballido, J. L. *et al.* A new giant titanosaur shed light on body mass evolution among sauropod dinosaurs. *R. Soc. B. Proc.* <https://doi.org/10.1098/rspb.2017.1219> (2017).
27. Wang, Y., You, H. & Wang, T. A new basal sauropodiform dinosaur from the Lower Jurassic of Yunnan Province. *China. Sci. Rep.* **7**, 41881. <https://doi.org/10.1038/srep41881> (2017).
28. Apaldetti, C., Martínez, R. N., Cerda, L., Pol, D. & Alcober, O. A. An early trend towards gigantism in Triassic sauropodomorph dinosaurs. *Nat. Eco. Evo.* **2**, 1227–1232. <https://doi.org/10.1038/s41598-018-0599-y> (2018).
29. McPhee, B. W., Benson, R. B. J., Botha-Brink, J., Bordy, E. M. & Choiniere, J. N. A giant dinosaur from the earliest Jurassic of South Africa and the transition to quadrupedality in early Sauropodomorphs. *Curr. Biol.* **8**, 15179. <https://doi.org/10.1016/j.cub.2018.07.063> (2018).
30. Pretto, F. A., Langer, M. C. & Schultz, C. L. A new dinosaur (Saurischia: Sauropodomorpha) from the Late Triassic of Brazil provides insights on the evolution of sauropodomorph body plan. *Zool. J. Linn. Soc.* **185**, 388–416 (2018).
31. Chapelle, K. E. J., Barrett, P. M., Botha, J. & Choiniere, J. N. *Ngwevu intloko*: A new early sauropodomorph dinosaur from the Lower Jurassic Elliot Formation of South Africa and comments on cranial ontogeny in *Massospondylus carinatus*. *PeerJ* **7**, e7240. <https://doi.org/10.7717/peerj.7240> (2019).
32. Peyre de Fabrègues, C. *et al.* A new species of early-diverging Sauropodiformes from the Lower Jurassic Fengjiahe Formation of Yunnan Province, China. *Sci. Rep.* **10**, 10961. <https://doi.org/10.1038/s41598-020-67754-4> (2020).
33. Pol, D., Otero, A., Apaldetti, C. & Martínez, R. N. Triassic sauropodomorph dinosaurs from South America and the origin and diversification of dinosaur dominated herbivorous faunas. *J. S. Am. Earth Sci.* **107**, 103145; <https://doi.org/10.1016/j.jsames.2020.103145> (2021).
34. Apaldetti, C., Pol, D. & Yates, A. M. The postcranial anatomy of *Coloradisaurus brevis* (Dinosauria: Sauropodomorpha) from the Late Triassic of Argentina and its phylogenetic implications. *Palaeontology* **56**, 277–301 (2013).
35. Yates, A. M., Bonnan, M. F., Neveling, J., Chinsamy, A. & Blackbeard, M. G. A new transitional sauropodomorph dinosaur from the Early Jurassic of South Africa and the evolution of sauropod feeding and quadrupedalism. *Proc. R. Soc. B Biol. Sci.* **277**, 787–794 (2010).
36. Otero, A., Krupandan, E., Pol, D., Chinsamy, A. & Choiniere, J. N. A new basal sauropodiform from South Africa and the phylogenetic relationships of basal sauropodomorphs. *Zool. J. Linn. Soc.* **174**, 589–634 (2015).
37. McPhee, B. W., Bonnan, M. F., Yates, A. M., Neveling, J. & Choiniere, J. N. A new basal sauropod from the pre-Toarcian Jurassic of South Africa: Evidence of niche-partitioning at the sauropodomorph–sauropod boundary?. *Sci. Rep.* **5**, 13224. <https://doi.org/10.1038/srep13224> (2015).
38. McPhee, B. W., Bordy, E. M., Sciscio, L. & Choiniere, J. N. The sauropodomorph biostratigraphy of the Elliot Formation of southern Africa: Tracking the evolution of Sauropodomorpha across the Triassic–Jurassic boundary. *Acta Palaeontol. Pol.* **62**, 441–465 (2017).
39. Button, D. J., Barrett, P. M. & Rayfield, E. J. Craniodental functional evolution in sauropodomorph dinosaurs. *Paleobiology* **43**, 435–462 (2017).
40. Bronzati, M., Müller, R. T. & Langer, M. C. Skull remains of the dinosaur *Saturnalia tupiniquim* (Late Triassic, Brazil): With comments on the early evolution of sauropodomorph feeding behaviour. *PLoS ONE* **14**(9), e0221387. <https://doi.org/10.1371/journal.pone.0221387> (2019).
41. Barrett, P. M. Paleobiology of herbivorous dinosaurs. *Ann. Rev. Earth and Planet. Sci.* **42**, 207–230 (2014).
42. Bonnan, M. F. & Yates, A. M. A new description of the forelimb of the basal sauropodomorph *Melanorosaurus*: Implications for the evolution pronation, manus shape and quadrupedalism in sauropod dinosaurs. *Spec. Pap. Palaeont.* **77**, 157–168 (2007).
43. McPhee, B. W., Yates, A. M., Choiniere, J. N. & Abdala, F. The complete anatomy and phylogenetic relationships of *Antetonitrus ingenipes* (Sauropodiformes, Dinosauria): Implications for the origins of Sauropoda. *Zool. J. Linn. Soc.* **171**, 151–205 (2014).
44. McPhee, B. W. & Choiniere, J. N. The osteology of *Pulanesaura eocollum*: Implications for the inclusivity of Sauropoda (Dinosauria). *Zool. J. Linn. Soc.* **182**, 830–861 (2017).
45. Foth, C., Sookias, R. B. & Ezcurra, M. D. Rapid initial morphospace expansion and delayed morphological disparity peak in the first 100 million years of the Archosauromorph evolutionary radiation. *Front. Earth Sci.* **9**, 723973. <https://doi.org/10.3389/feart.2021.723973>
46. Griffin, D. *et al.* An exceptional new Late Triassic (Carnian) fossil assemblage from Zimbabwe and the biogeography of the early dinosaurs across Pangea. *Meeting program and abstracts, 78th Annual Meeting of the Society of Vertebrate Paleontology*, 137 (2018).
47. Novas, F. E., Ezcurra, M. D., Chatterjee, S. & Kutty, T. S. New dinosaur species from the Upper Triassic Upper Maleri and Lower Dharmaram formations of Central India. *Earth Environ. Sci. Trans. R. Soc. Edinb.* **101**, 333–349 (2011).
48. Ballell, A., Rayfield, E. J. & Benton, M. Osteological redescription of the Late Triassic sauropodomorph dinosaur *Thecodontosaurus antiquus* based on new material from Tytherington, southwestern England. *J. J. Vertebr. Paleontol.* <https://doi.org/10.1080/02724634.2020.1770774> (2020).
49. Marsicano, C. A., Irmis, R. B., Mancuso, A. C., Mundil, R. & Chemale, F. The precise temporal calibration of dinosaur origins. *Proc. Nat. Acad. Sci.* **113**, 509–513 (2015).
50. Benson, R. B. J. *et al.* Rates of dinosaur body mass evolution indicate 170 million years of sustained ecological innovation on the avian stem lineage. *PLoS Biol.* **12**, e1001853. <https://doi.org/10.1371/journal.pbio.1001853> (2014).
51. Barrett, P. M. & Upchurch, P. The evolution of feeding mechanisms in early sauropodomorph dinosaurs. *Spec. Pap. Palaeontol.* **77**, 91–112 (2007).
52. Martínez, R. N. *et al.* A basal dinosaur from the dawn of the dinosaur era in southwestern Pangaea. *Science* **331**, 201–210 (2011).
53. Desojo, J. B. *et al.* The Late Triassic Ischigualasto Formation at Cerro Las Lajas (La Rioja, Argentina): Fossil tetrapods, high-resolution chronostratigraphy and faunal correlations. *Sci. Rep.* **10**, 12784. <https://doi.org/10.1038/s41598-020-67854-1> (2020).
54. Martínez, R. N. *et al.* A new Late Triassic vertebrate assemblage from Northwestern Argentina. *Ameghiniana* **52**, 379–390 (2015).

55. Rauhut, O. W. M., Fechner, R., Remes, K. & Reis, K. How to get big in the Mesozoic: The evolution of the sauropodomorph body plan. In *Biology of the Sauropod Dinosaurs: Understanding the Life of Giants. Life of the Past* (eds. Klein, N., Remes, K., Gee, C. T. & Sander, P. M.) 119–149 (Indiana University Press, 2011).
56. Nesbitt, S. J., Irmis, R. B. & Parker, W. G. A critical reevaluation of the Late Triassic dinosaur taxa of North America. *J. Syst. Palaeontol.* **5**, 209–243 (2007).
57. Mannion, P. D. & Upchurch, P. Completeness metrics and the quality of the sauropodomorph fossil record through geological and historical time. *Paleobiology* **36**, 283–302 (2010).
58. Mannion, P. D., Upchurch, P., Carrano, M. T. & Barrett, P. M. Testing the effect of the rock record on diversity: A multidisciplinary approach to elucidating the generic richness of sauropodomorph dinosaurs through time. *Biol. Rev.* **86**, 157–181 (2011).
59. Barrett, P. M. Prosauropod dinosaurs and iguanas: Speculations on the diets of extinct reptiles. In *Evolution of herbivory in terrestrial vertebrates. Perspective from the fossil record* (ed. Sues, H.-D.) 42–78 (Cambridge University Press, Cambridge, 2000).
60. Upchurch, P. & Barrett, P. M. A phylogenetic perspective on sauropod diversity. In *The Sauropods: Evolution and paleobiology* (eds. Curry-Rogers, K. A. & Wilson, J. A.) 104–124 (University of California Press, California, 2005).
61. Pradelli, L. A., Learidi, J. M. & Ezcurra, M. D. Body size disparity of the Archosauromorph reptiles during the first 90 million years of their evolution. *Ameghiniana* <https://doi.org/10.5710/AMGH.16.09.2021.3441> (2021).
62. Bonaparte, J. F. Evolución de las vértebras presacras en Sauropodomorpha. *Ameghiniana* **36**, 115–187 (1999).
63. Wilson, F. A. Vertebral laminae in sauropods and other saurischian dinosaurs. *J. Vertebr. Paleontol.* **18**, 639–653 (1999).
64. Sander, P. M., Klein, N., Stein, K. & Wings, O. Sauropod bone histology and its implications for sauropod biology. In *Biology of the Sauropod Dinosaurs* (eds. Klein, N., Remes, K., Gee, C. T. & Sander, P. M.) (Indiana University Press, 2011).
65. Cúneo, R. *et al.* High-precision U-Pb geochronology and a new chronostratigraphy for the Cañadón Asfalto Basin, Chubut, central Patagonia: Implications for terrestrial faunal and floral evolution in Jurassic. *Gondwana Res.* **24**, 1267–1275 (2013).
66. Goloboff, P. A. & Catalano, S. A. TNT version 1.5, including a full implementation of phylogenetic morphometrics. *Cladistics* **32**, 221–238 (2016).
67. Bapst, D. W. Paleotree: An R package for paleontological and phylogenetic analyses of evolution. *Meth. Ecol. Evol.* **3**, 803–807 (2012).
68. Laurin, M. The evolution of body size, Cope's rule and the origin of amniotes. *Syst. Biol.* **53**, 594–622 (2004).
69. Lloyd, G. T. Estimating morphological diversity and tempo with discrete character-taxon matrices: Implementation, challenges, progress, and future directions. *Biol. J. Linn. Soc.* **118**, 131–151 (2016).
70. Ezcurra, M. D. & Butler, R. J. The rise of the ruling reptiles and ecosystem recovery from the Permo-Triassic mass extinction. *Proc. R. Soc. B Biol. Sci.* **285**, 20180361. <https://doi.org/10.1098/rspb.2018.0361> (2018).
71. Flannery Sutherland, J. T., Moon, B. C., Stubbs, T. L. & Benton, M. J. Does exceptional preservation distort our view of disparity in the fossil record?. *Proc. R. Soc. B* **286**, 20190091 (2019).
72. Lehmann, O. E., Ezcurra, M. D., Butler, R. J. & Lloyd, G. T. Biases with the Generalized Euclidean Distance measure in disparity analyses with high levels of missing data. *Palaeontology* **62**, 837–849 (2019).
73. Guillerme, T., Puttick, M. N., Marcy, A. E. & Weisbecker, V. Shifting spaces: Which disparity or dissimilarity measurement best summarize occupancy in multidimensional spaces?. *Ecol. Evol.* **10**, 7261–7275 (2020).
74. Lehmann, O. E. & Ezcurra, M. D. Desafíos en los análisis de disparidad con taxones incompletos: el caso de la Máxima Distancia Observada Rescalada (MORD). *Reunión de Comunicaciones de la Asociación Paleontológica Argentina, Libro de Resúmenes*, 125–126 (2020).
75. Guillerme, T. DisRity: A modular R package for measuring disparity. *Meth. Ecol. Evol.* **9**, 1755–1763 (2018).
76. Oksanen, J. *et al.* vegan: Community Ecology Package. R package version 2.5–6. <https://CRAN.R-project.org/package=vegan> (2019).
77. Revell, L. J. phytools: An R package for phylogenetic comparative biology (and other things). *Meth. Ecol. Evol.* **3**, 217–223 (2012).
78. Adams, D. C. A method for assessing phylogenetic least squares models for shape and other high-dimensional multivariate data. *Evolution* **68**, 2675–2688 (2014).
79. Adams, D., Collyer M., Kaliontzopoulou A. & Baken E. Geomorph: Software for geometric morphometric analyses. R package version 4.0. <https://CRAN.R-project.org/package=geomorph> (2021).
80. Campione, N. E. & Evans, D. C. An universal scaling relationship between body mass and proximal limb bone dimensions in quadrupedal terrestrial tetrapods. *BMC Biol.* **10**, 60 (2012).

Acknowledgements

Oscar Lehmann for discussion about the resampled results of volume disparity metrics. Thomas Guillerme and Jonah Choiniere for their comments that notably improved this manuscript. The research was funded by the Agencia Nacional de Promoción Científica y Tecnológica—FONCYT (Grant numbers 2016-0236 C.A., 2014-1288 D.P., 2015-0711 R.N.M., 2018-01186 M.D.E.); Secretaría de Ciencia e Innovación, Gobierno de San Juan (SECITI to R.N.M.); Sepkoski Grant 2020 (C.A.). TNT v.1.5 is freely available through the Willi Hennig Society.

Author contributions

C.A. and D.P. designed the research project and made the figures. M.D.E. conducted the statistical analyses. All authors contributed to the text of the manuscript.

Competing interests

The authors declare no competing interests.

Additional information

Supplementary Information The online version contains supplementary material available at <https://doi.org/10.1038/s41598-021-01120-w>.

Correspondence and requests for materials should be addressed to C.A.

Reprints and permissions information is available at www.nature.com/reprints.

Publisher's note Springer Nature remains neutral with regard to jurisdictional claims in published maps and institutional affiliations.



Open Access This article is licensed under a Creative Commons Attribution 4.0 International License, which permits use, sharing, adaptation, distribution and reproduction in any medium or format, as long as you give appropriate credit to the original author(s) and the source, provide a link to the Creative Commons licence, and indicate if changes were made. The images or other third party material in this article are included in the article's Creative Commons licence, unless indicated otherwise in a credit line to the material. If material is not included in the article's Creative Commons licence and your intended use is not permitted by statutory regulation or exceeds the permitted use, you will need to obtain permission directly from the copyright holder. To view a copy of this licence, visit <http://creativecommons.org/licenses/by/4.0/>.

© The Author(s) 2021